ENGINEERING RESEARCH

ENGINEERING RESEARCH

ENGINEERING RESEARCH

ENGINEERING RESEARCH

ENGINEERING RESEARCH

PROGRESS REPORT

APPLICATION OF BLADE-ELEMENT TECHNIQUES TO DESIGN AND PERFORMANCE PREDICTION PROBLEMS FOR AXIAL-FLOW TURBOMACHINERY

T. H. Okiishi – Principal Investigator
M. J. Miller – Research Associate
P. Kavanagh – Principal Investigator
G. K. Serovy – Project Director

April 1, 1969 – September 30, 1969

This project is supported by the National Aeronautics and Space Administration through NASA Grant NGL 16-002-005 and is a part of the Turbomachinery Components Research Program of the Engineering Research Institute.

ERI-61400
Project 407S

ENGINEERING RESEARCH INSTITUTE
IOWA STATE UNIVERSITY AMES

APPLICATION OF BLADE-ELEMENT TECHNIQUES TO DESIGN AND PERFORMANCE PREDICTION PROBLEMS FOR AXIAL-FLOW TURBOMACHINERY

T. H. Okiishi, M. J. Miller, P. Kavanagh and G. K. Serovy

INTRODUCTION

Research directed toward developing improved methods for hydrodynamic design and prediction of performance of axial-flow pumps is underway at Iowa State University. This research is supported by the National Aeronautics and Space Administration through Grant NGL 16-002-005. Progress from April 1, 1969 through September 30, 1969 is outlined in this report.

To expedite the data correlation associated with empirical prediction of axial-flow pump deviation angles and total-head loss coefficients, isolated rotor data for eleven different axial-flow pump rotor configurations were organized and stored on magnetic tape in a uniform format so that retrieval for data analysis would be simplified. A summary of the data considered is included in this report. Tests of three of several approaches to correlation of deviation angle data are discussed. Preliminary conclusions associated with total-head loss coefficient correlation development are also mentioned.

PUMP ROTOR DATA ORGANIZATION

Table I lists descriptions of eleven different axial-flow pump rotor configurations. Non-cavitating operation data obtained at the Lewis Research Center-NASA, for each of these rotors, were uniformly stored on magnetic tape to form an organized source of data to serve as a base for tests of proposed empirical deviation angle and total-head loss coefficient prediction methods. The system for testing prediction methods is organized so that the correlation parameters associated with any proposed prediction method can be calculated and displayed graphically for quick evaluation.

Table I. NASA axial-flow pump rotor configuration descriptions.[a]

NASA configuration number	Tip diameter, inches	r_H/r_T	Number of blades	Blade section profile [b]	Blade chord length,[c] inches	Radial tip clearance,[d] inches	Design tip section D-factor	Design point flow coefficient
02	9.0	0.4	16	DCA	1.5	0.013 – 0.020	0.23	0.293
07	9.0	0.7	19	DCA	1.5	0.005 – 0.012	0.43	0.294
09	9.0	0.7	8	DCA	3.04	0.013 – 0.020	0.46	0.294
5	9.0	0.8	19	DCA	1.5	0.015 – 0.017	0.66	0.466
6	9.0	0.8	19	DCA	1.5	0.025 – 0.027	0.66	0.466
8	5.0	0.8	19	DCA	0.834	0.007 – 0.009	0.66	0.466
9	5.0	0.8	19	DCA	0.834	0.015 – 0.017	0.66	0.466
10	5.0	0.8	19	DCA	0.834	0.022 – 0.024	0.66	0.466
13	9.0	0.85	33	DCA	1.172	0.009 – 0.011	0.72	0.5
14	9.0	0.9	19	DCA	1.5	0.009 – 0.011	0.63	0.7
16	9.0	0.85	33	CUBIC	1.172	0.009 – 0.011	0.72	0.5

[a]All rotors were tested without inlet guide vanes and downstream stator blades.

[b]DCA indicates a DOUBLE CIRCULAR ARC blade section profile.

[c]All blade chord lengths were uniform along the blade span.

[d]The range of circumferential variation of radial tip clearance is indicated.

DEVIATION ANGLE

At the beginning of the report period, after a review of pertinent literature and consultations with NASA personnel, several methods of accounting for the effect of varying axial velocity ratio were selected as promising for correlation of the NASA axial flow pump rotor deviation angle data. Three approaches have been tested with the data for the eleven configurations of Table I. The first two approaches differ in only one detail and thus will be described together. The basic idea was to calculate an equivalent outlet velocity diagram having an axial velocity ratio of 1.0 (AVR = 1). In approach I, the equivalent diagram was obtained by assuming $V_{z,2,eq} = V_{z,1}$, $U_{2,eq} = U_2$, and $V'_{\theta,2,eq} = V'_{\theta,2}$. The last condition amounts to assuming the circulation relative to the blade section remains constant, an assumption which has been widely recommended in one form or another (Refs. 1 – 4). In approach II the condition of equal circulation was replaced by the requirement that the D-factors computed from the equivalent diagram and the measured diagram be equal as follows.

$$1 - \frac{V'_2}{V'_1} + \frac{r_2 V'_{\theta,2} - r_1 V'_{\theta,1}}{(r_1 + r_2)\,\sigma\, V'_1} = 1 - \frac{V'_{2,eq}}{V'_1} + \frac{r_2 V'_{\theta,2,eq} - r_1 V'_{\theta,1}}{(r_1 + r_2)\,\sigma\, V'_1} \qquad (1)$$

which can be reduced to

$$- V'_2 + \frac{V'_{\theta,2}}{2\sigma} = - V'_{2,eq} + \frac{V'_{\theta,2,eq}}{2\sigma} \qquad (2)$$

when

$$r_1 = r_2 \qquad (3)$$

rearranging

$$V'_{\theta,2,eq} = 2\sigma\,(V'_{2,eq} - V_2) + V_{\theta,2} \tag{4}$$

substituting (4) into (5)

$$(V'_{2,eq})^2 = (V'_{\theta,2,eq})^2 + (V_{z,1})^2 \tag{5}$$

yields a quadratic equation in $V'_{2,eq}$. The equivalent diagram can then be computed from the appropriate root $V_{2,eq}$, U_2, and $V_{z,1}$.

In both cases the resulting equivalent relative flow angle $\beta'_{2,eq}$ was used in an iterative procedure to determine an equivalent camber. The equivalent camber was required to satisfy the following relation

$$\phi^o_{eq} = \kappa_1 - \kappa_{2,eq} \tag{6}$$

where

$$\kappa_{2,eq} = \beta'_{2,eq} - \delta_{eq} \tag{7}$$

$$\delta_{eq} = m\,\phi^o_{eq}/\sigma^{\frac{1}{2}} \tag{8}$$

That is, an equivalent camber was obtained such that the sum of the corresponding outlet blade angle and the deviation angle obtained using the equivalent camber in Carter's rule was equal to the relative flow angle in the equivalent outlet velocity diagram. (See Fig. 5. for blade nomenclature.) The expectation was that δ_{eq} would more closely approximate the measured deviation angle than a value computed directly from Carter's rule using the actual blade section camber. However, the comparison of results in Fig. 1 shows that the equivalent deviation angles are generally smaller than the deviation angle from Carter's rule which itself is much too small over most of the blade for the high loaded rotors in Fig. 1(b) and 1(c). These results are typical for all the rotor configurations and for other flows. Based on these results these two correlation approaches will be discarded.

Preliminary results from the third approach are considered substantially more promising. This approach is similar to approach I discussed above except that the camber term in the function used to compute δ_{eq} has a variable exponent.

$$\delta_{eq} = m\ (\phi^{o}_{eq})^{b}/\sigma^{\frac{1}{2}} \quad . \qquad (9)$$

In this case the exponent was chosen so that

$$\delta_{eq} = \delta_{exp} \quad . \qquad (10)$$

Preliminary values of the exponent b as a function of axial velocity ratio are shown in Fig. 2 for the eleven configurations at ten percent of the passage height from the tip. These values were obtained using data which corresponded closely to two-dimensional reference incidence angle operation. With two exceptions, which represent rather unusual geometries, a constant value of 1.1 approximates the data well. The trends for other radial positions are similar except near the hub where inconsistencies appear. These preliminary results appear promising, but further analysis is considered necessary to evaluate the effect of possible errors in the measured axial velocities on the correlation. This work is currently

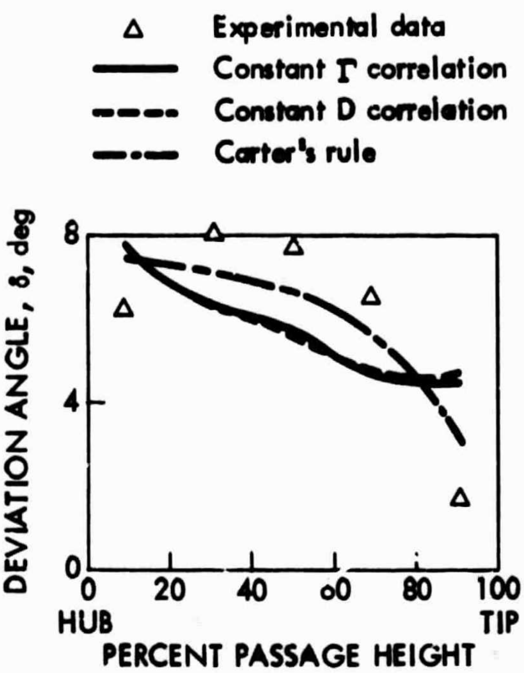

1(a), 0.7 hub-tip radius rotor, N = 3600 rpm, $\overline{\phi}$ = 0.284, NASA config. 07.

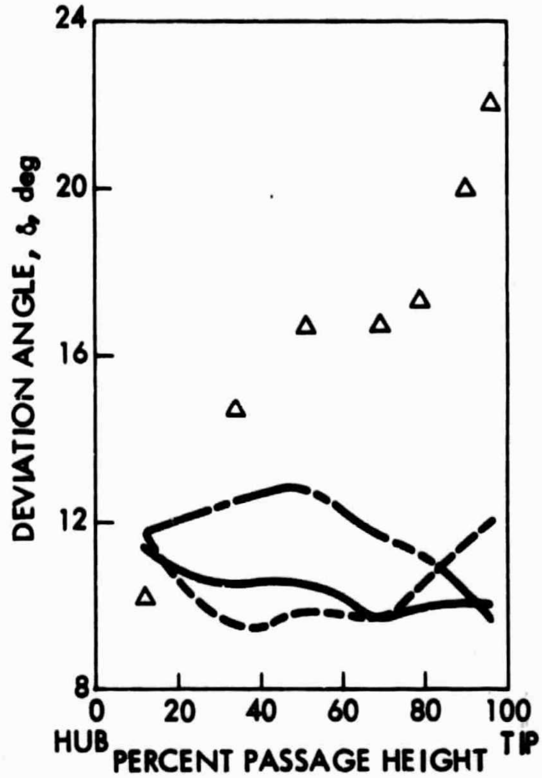

1(b), 0.8 hub-tip radius ratio, N = 3000 rpm, $\overline{\phi}$ = 0.451, NASA config. 5.

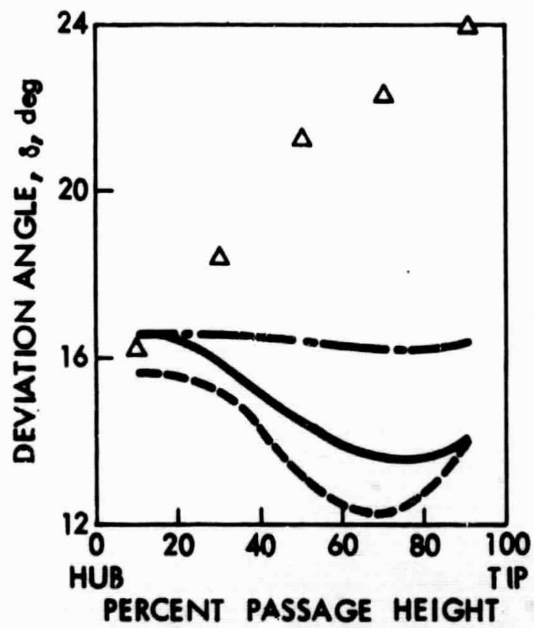

1(c), 0.9 hub-tip radius ratio, N = 2500 rpm, $\overline{\phi}$ = 0.698, NASA config. 14.

Fig. 1. Deviation angle spanwise distribution comparisons.

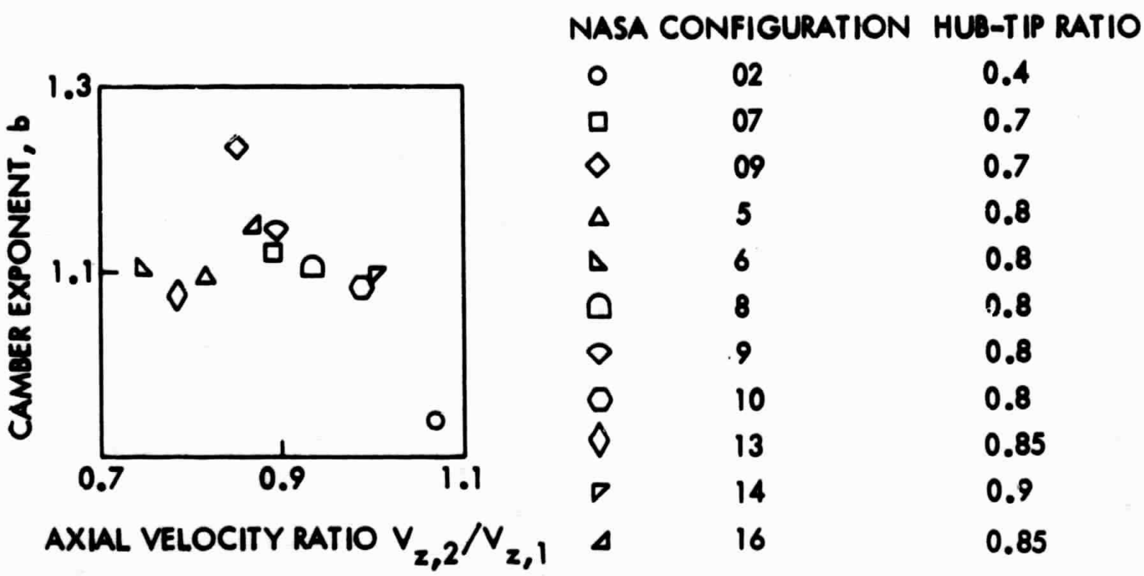

Fig. 2. Camber exponent for sections ten percent of passage height from tip at reference incidence angle (2-D).

under way and might clarify the trends of exponent b calculated near the hub. The next step will be an attempt to obtain a correlation accounting for incidence angle change.

BLADE-ELEMENT TOTAL PRESSURE LOSS COEFFICIENT PREDICTION

Several parameter forms related to the blade-element flow model wake thickness (θ/c) and loading (D or DEQ) were tested for suitability as correlation parameters with the experimental data of the pump rotors described in Table I. The following versions of the ratio of blade-element wake momentum thickness to chord length were tested:

$$\left(\frac{\theta}{c}\right)_a = \frac{\bar{\omega} \cos \beta_2'}{2\sigma} \tag{11}$$

$$\left(\frac{\theta}{c}\right)_b = \frac{\bar{\omega} \cos^3 \beta_2'}{2\sigma \cos^2 \beta_1'} \left(\frac{V_{z,1}}{V_{z,2}}\right)^3 \left(\frac{3H_2 - 1}{2H_2}\right) \tag{12}$$

$$\left(\frac{\theta}{c}\right)_c = \frac{\bar{\omega}}{2\sigma} \left(\frac{V_1'}{V_2'}\right)^2 \cos \beta_2' \tag{13}$$

$$\left(\frac{\theta}{c}\right)_d = \frac{\bar{\omega} \cos \beta_2'}{2\sigma} \left(\frac{\cos \beta_2'}{\cos \beta_1'}\right)^2 . \tag{14}$$

Note that $(\theta/c)_c$ and $(\theta/c)_d$ are "abbreviated" forms of Lieblein's relationship for (θ/c) for two-dimensional cascade flow as follows:

$$\left(\frac{\theta}{c}\right)_{2-D} = \frac{\bar{\omega} \cos \beta_2}{2\sigma} \left(\frac{\cos \beta_2}{\cos \beta_1}\right)^2 \left(\frac{3H_2 - 1}{2H_2}\right) \left(1 - \left(\frac{\theta}{c}\right)_{2-D} \frac{\sigma H_2}{\cos \beta_2}\right)^3 . \tag{15}$$

The derivation of the relationship for $(\theta/c)_b$ is found in Ref. 6 .

The following relationships for D and DEQ were tested:

$$D = 1 - \frac{V'_2}{V'_1} + \frac{|r_1 V'_{\theta,1} - r_2 V'_{\theta,2}|}{\sigma V'_1 (r_1 + r_2)} \tag{16}$$

$$DEQ = \frac{V_{z,1}}{V_{z,2}} \frac{\cos \beta'_2}{\cos \beta'_1} \left\{ C_1 + C_2 |i - i^*_{2-D}|^{C_3} + C_4 \frac{\cos^2 \beta_1}{\sigma V_{z,1}} \left(V'_{1,\theta} - V'_{2,\theta} \frac{r_2}{r_1} \right) \right\} \tag{17}$$

with C_1, C_2, C_3 and C_4 based on Lieblein's (5) two-dimensional cascade correlation. Note that D and DEQ are based on relative circulation, Γ'.

While no combination of the different versions of the blade-element wake momentum thickness to chord ratio (θ/c) and loading parameter (D or DEQ) proved to be completely adequate as tested, several combinations showed potential for further development and definite improvement over the loss-prediction method presently used in the Iowa State University axial-flow pump analysis program. In general, the tested parameters seemed to work best near the tip as indicated, for example, in Figs. 3 and 4.

Work in the immediate future on correlating experimental total-pressure loss data will include more suitability tests of the different versions of (θ/c), D and DEQ involving variation of H_2, C_1, C_2, C_3 and C_4 and development of improved blade-element loading and wake thickness parameters.

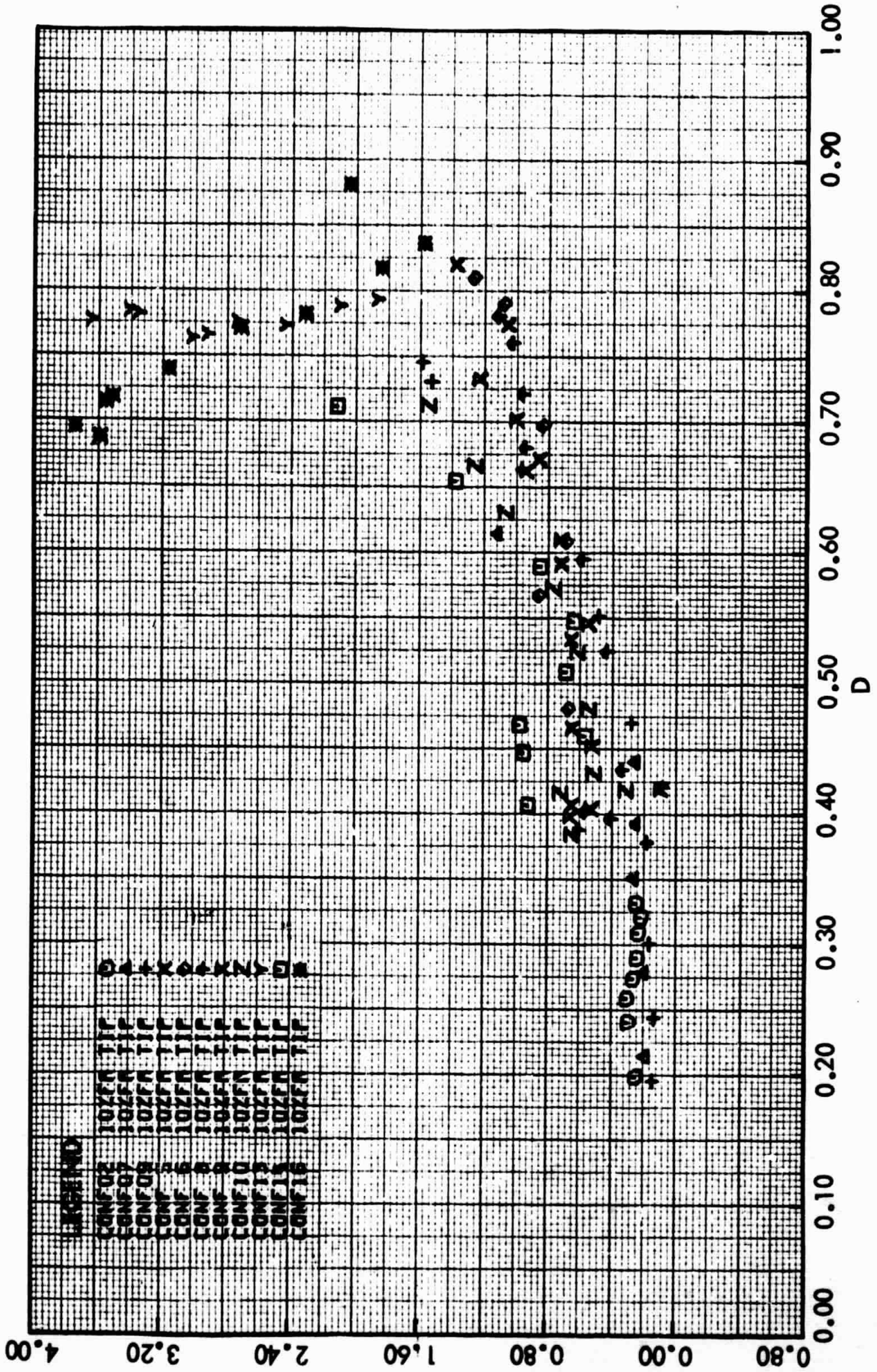

Fig. 3. Variation of $(\theta/C)_d$ with D near tip.

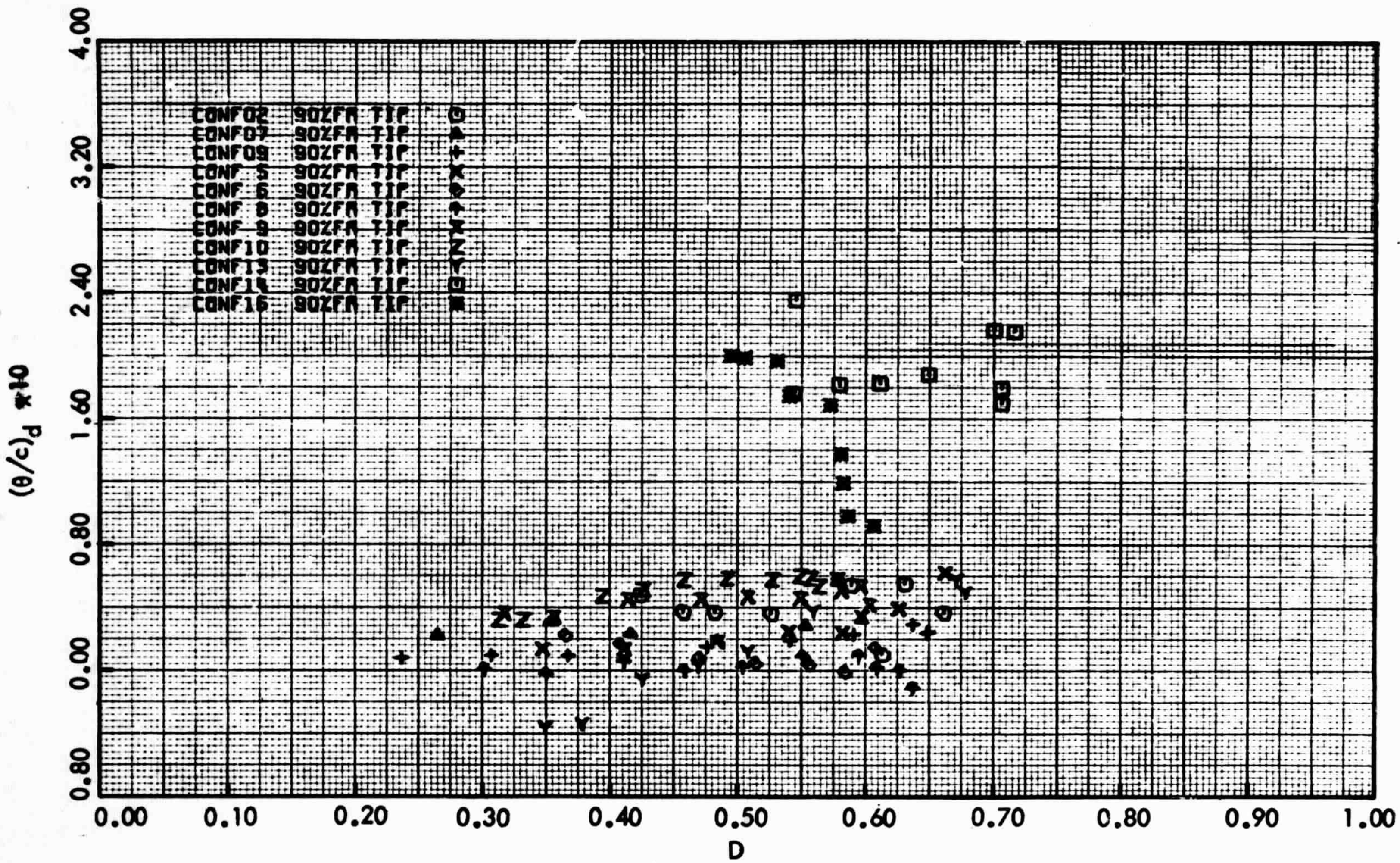

Fig. 4. Variation of $(\theta/C)_d$ with D near hub.

SYMBOLS

b	camber exponent
c	chord length (Fig. 5)
C_1, C_2, C_3, C_4	empirical coefficients in equivalent diffusion factor equation
D	diffusion factor
DEQ	equivalent diffusion factor
H_2	blade-element wake shape factor
m	parameter in deviation angle relationship radius
r	radius
U	blade velocity
V	fluid velocity
β	fluid flow angle (Fig. 5)
Γ	circulation
δ	deviation angle
θ	wake momentum thickness
κ	blade angle (Fig. 5)
σ	solidity
ϕ^o	camber angle (Fig. 5)
$\bar{\omega}$	total-head loss coefficient

Subscripts:

1	inlet location
2	exit location
eq	equivalent
exp	experimental

z	axial component
θ	tangential component

Superscript:

'	relative to coordinates moving with rotor

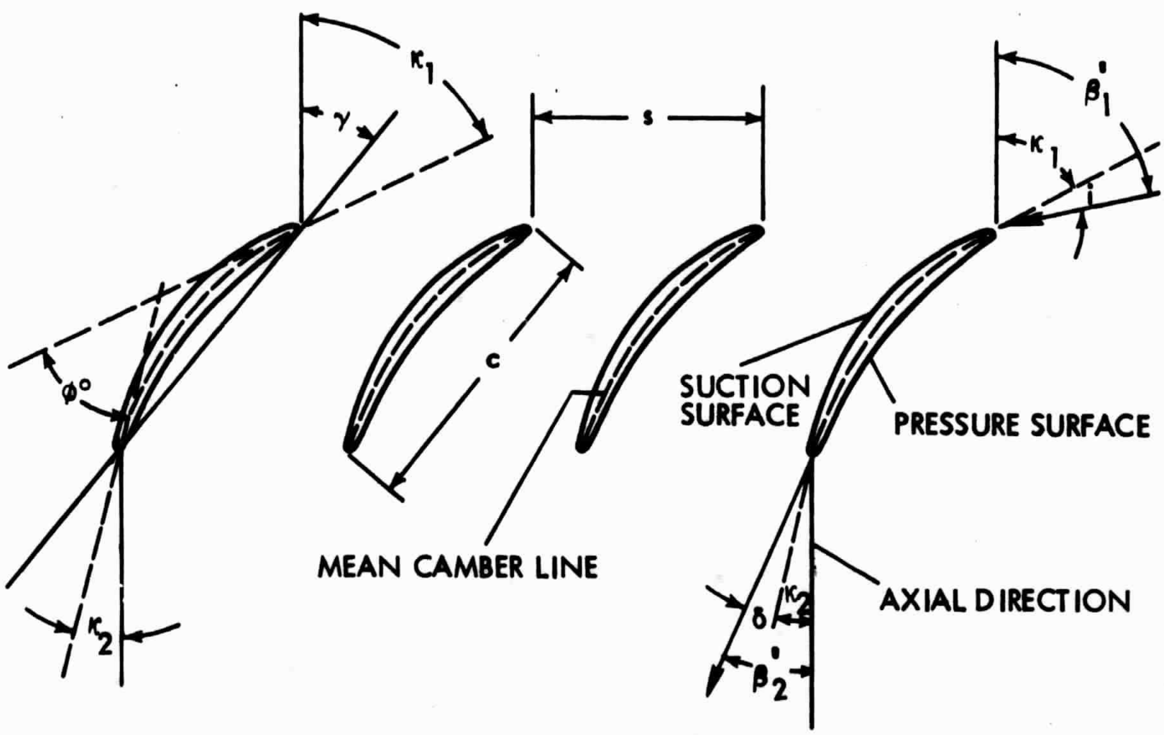

Fig. 5. Two-dimensional cascade view and blade nomenclature.

REFERENCES

1. Erwin, John R.; and Emery, James C.: Effect of Tunnel Configuration and Testing Technique on Cascade Performance. US National Advisory Committee for Aeronautics Report 1016, 1951.

2. Schulze, Wallace M.; Erwin, John R.; and Ashby, George C.: NACA 65-series Compressor Rotor Performance with Varying Annulus-Area Ratio, Solidity, Blade Angle, and Reynolds Number and Comparisons with Cascade Results US National Advisory Committee for Aeronautics Technical Note 4130, 1957.

3. Jansen, W.; and Moffatt, W. C.: The Off-Design Analysis of Axial-Flow Compressors. American Society of Mechanical Engineers Transactions, Series A: Journal of Engineering for Power 89: 453-462. 1967.

4. Scholz, N.: Two-Dimensional Correction of the Outlet Angle in Cascade Flow. J. of the Aeronautical Sciences, Readers Forum, 20: 786–787, 1953.

5. Lieblein, S.: Loss and Stall Analysis of Compressor Cascades. American Society of Mechanical Engineers Transactions, Series D: Journal of Basic Engineering 81: 387–400, 1959.

6. Okiishi, T. H.; Miller, M. J.; Kavanagh P.; and Serovy, G. K.: Application of Blade Element Techniques to Design and Performance Prediction Problems for Axial-Flow Turbomachinery. Progress Report, Iowa State University, Engineering Research Institute, ERI-485, 1969.

KK/mn